Electronic Supplementary Material (ESI) for Nanoscale.


Supporting Information

# Synthetic Azobenzene-Containing Metal-Organic Framework Ion Channels Toward Efficient Light-Gated Ion transport at the Subnanoscale

Tianyue Qian, [a] Chen Zhao, [b] RuoxinWang, [a] Xiaofang Chen, [a] Jue Hou, [c] Huanting Wang*[a] and Huacheng Zhang*[b]

a. Department of Chemical Engineering, Monash University, Clayton, Victoria 3800, Australia. Email: huanting.wang@monash.edu
b. Chemical and Environmental Engineering, School of Engineering, RMIT University, Melbourne, Victoria 3000, Australia. Email: huacheng.zhang@rmit.edu.au.
c. Manufacturing, CSIRO, Clayton, Victoria 3168, Australia.

## 1. Supplementary Figures

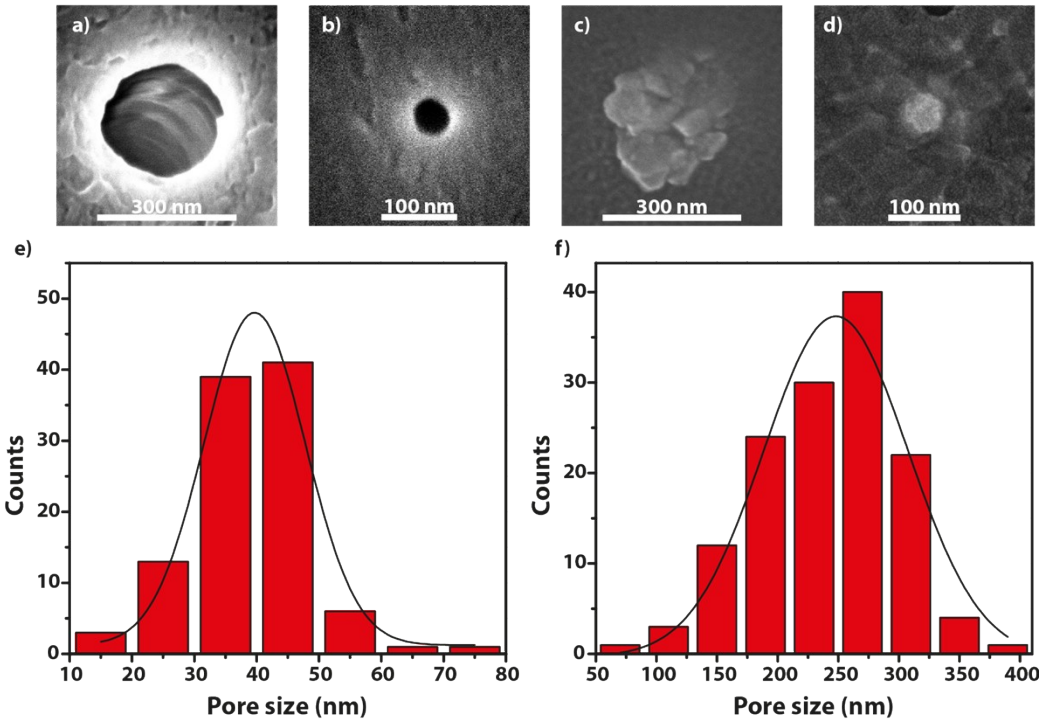


Figure S1. Structural characterization of bullet-shaped nanochannels. (a, b) SEM image of the (a) base side and (b) the tip side of PET nanochannel with a scale bar of 300 and 100 nm. (c, d) SEM image of (c) the base side and (d) the tip side of PET-UiO-66 nanochannel, with a scale bar of 300 and 100 nm. (e) Tip radius distribution, which has an average value of 39±9 nm. (f) Base radius distribution, which has an average value of 242±56 nm.

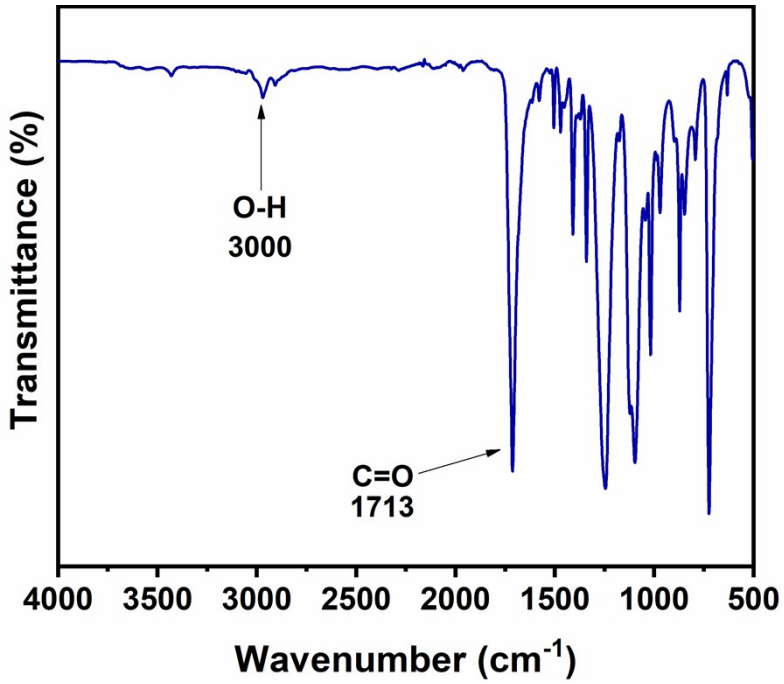


Figure S2. FTIR spectrum of the PET nanochannel membrane.

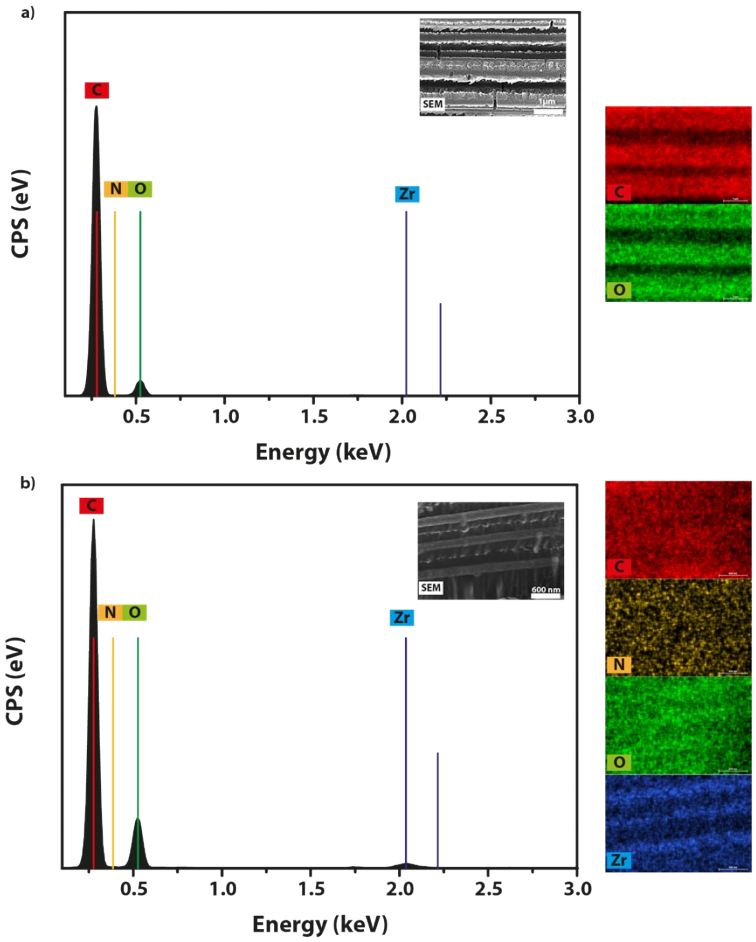


Figure S3. Characterization of the nanochannels. (a) EDX spectrum of a multiple nanochannel PET membrane (with a pore density of $10^8$ $cm^{-2}$) with the insets of an SEM cross-sectional image of t the PET multi-nanochannel membrane, and the EDX carbon (C, red) and oxygen (O, green) mappings; the scale bars are 1 μm. (c) EDX spectrum of a PET-UiO-66 nanochannel membrane (with a pore density of $10^8$ $cm^{-2}$) with the insets of an SEM cross-sectional image of the middle part of the PET multi-nanochannel membrane, and the EDX carbon (C, red), nitrogen (N, yellow), oxygen (O, green), zirconium (Zr, blue) mappings along the cross section of the membrane; the scale bars are 600 nm.

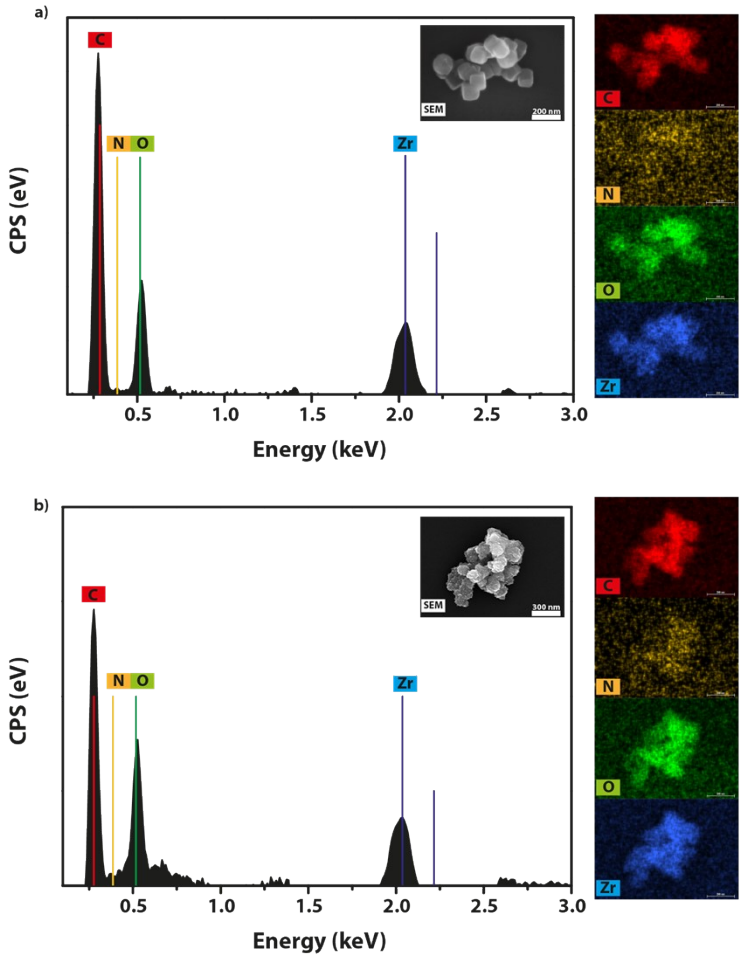


Figure S4. Characterization of MOF particles. (a) EDX spectrum of UiO-66 crystals along with the insets of an SEM cross-sectional image of the PET multi-nanochannel membrane, and the EDX carbon (C, red), nitrogen (N, yellow), oxygen (O, green), zirconium (Zr, blue) mappings along the cross section of the membrane; the scale bars are 200 nm. (b) EDX spectrum of a UiO-66-AZODC-2:1 crystal with the insets of an SEM cross-sectional image of the PET multi-nanochannel membrane, and the EDX carbon (C, red), nitrogen (N, yellow), oxygen (O, green), zirconium (Zr, blue) mappings; the scale bars are 300nm.

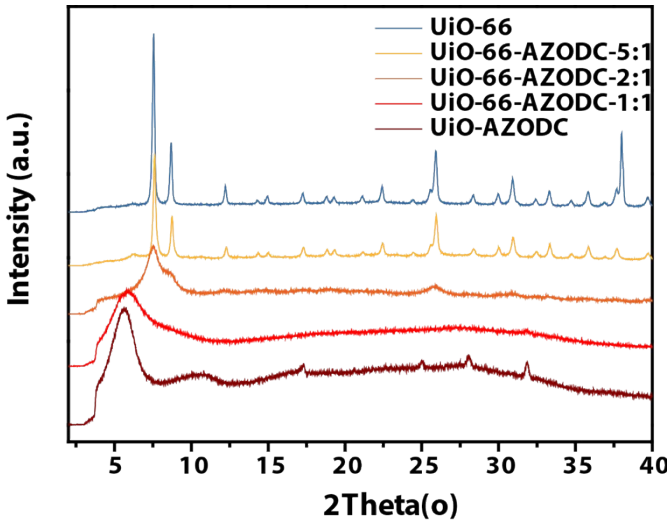


Figure S5. Powder X-ray diffraction (PXRD) patterns of UiO-66 crystals, UiO-66-AZODC mixed ligand MOFs and UiO-AZODC crystals.

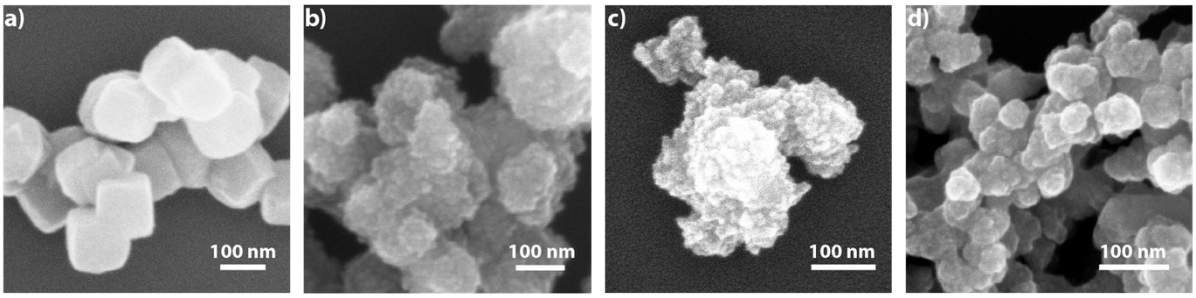


Figure S6. SEM image of MOF particles. (a) SEM image UiO-66 particles. (b,c) SEM image of the mixed-ligand UiO-66-AZODC MOF particles with different ratios of ligands added. The ratio of BDC ligands to AZODC ligands are (b) 2:1 and (c)1:1, respectively. (d) SEM image UiO-AZODC MOF particles.

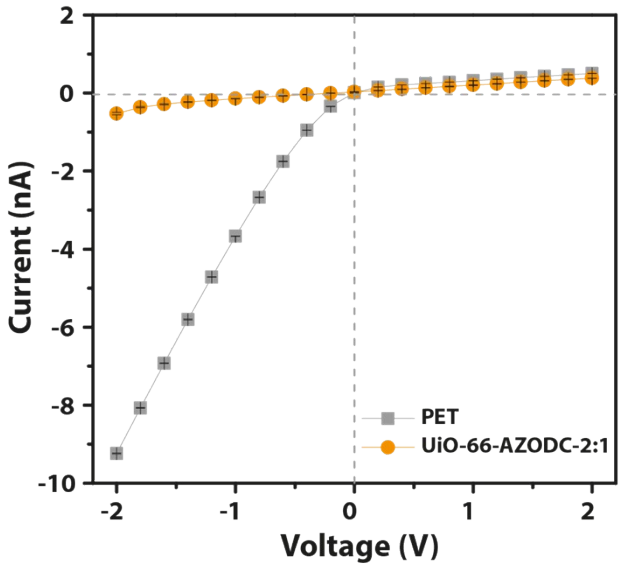


Figure S7. Ion transport properties. I-V curves of the PET nanochannels before and after the in-situ growth of UiO-66-AZODC.

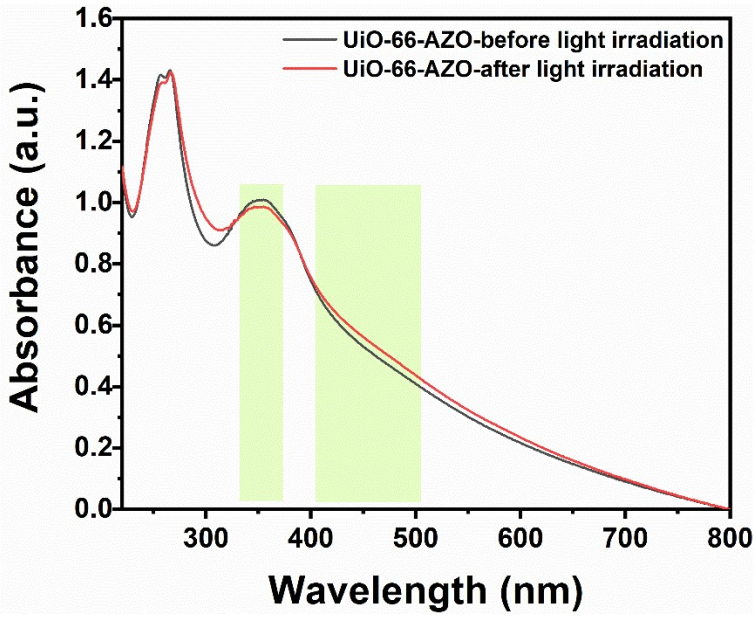


Figure S8. The UV-Vis spectra of UiO-66-AZODC-2:1 MOF powders before and after UV light (365 nm) irradiation in water

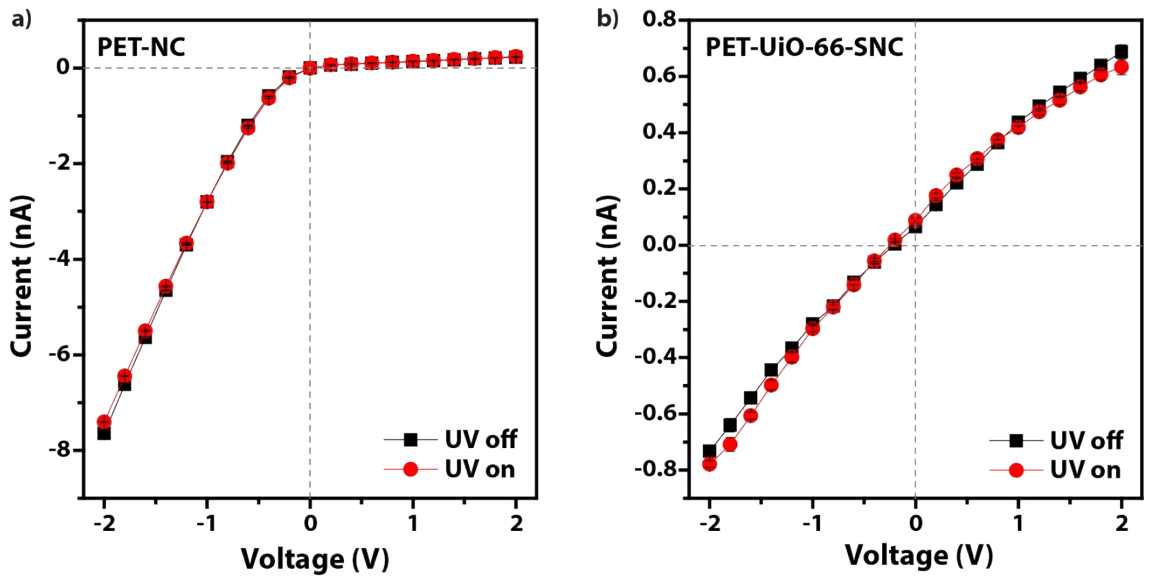


Figure S9. Ion transport properties of the reference sample. I-V curves of the PET-NC and UiO-66 SNC with UV light off and on.

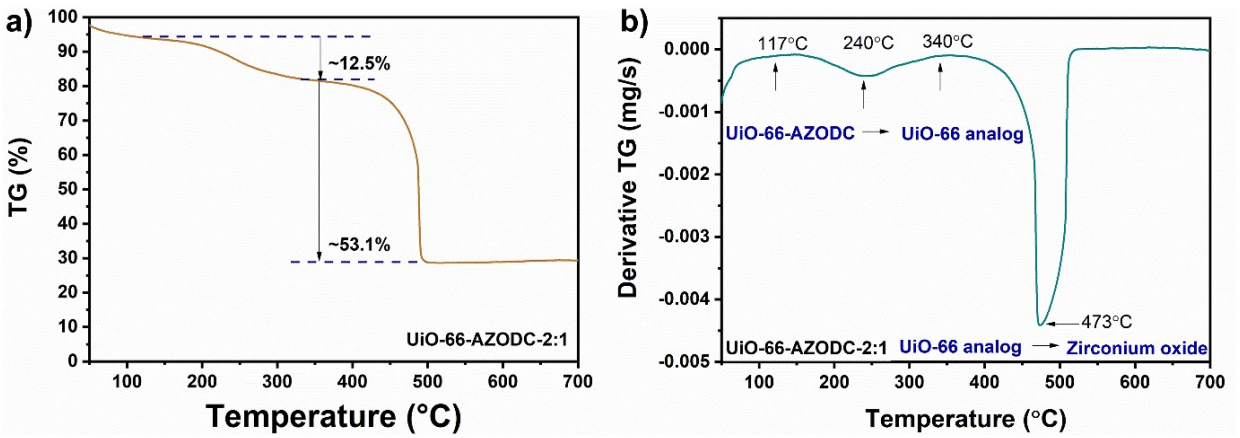


Figure S10. TG (a) and derivative TG (b) curves of UiO-66-AZODC-2:1.

As shown in the above figure, based on the melting point differences (AZODC>117°C, BDC>300°C), the combustion of UiO-66-AZODC-2:1 includes the evaporation of water/solvent molecules at the initial period (before 117°C), the degradation of AZODC (117°C~340°C, peak at 240°C), the oxidation of BDC and the final transformation into zirconium oxide (>340°C, peak at 473°C). Therefore, the weight loss of ~12.5% is attributed to AZODC mass fraction, and its molar ratio can be calculated using the following equation:

the molar ratio of AZODC = AZODC mole number/UiO-66-AZODC mole number= (AZODC mass fraction/AZODC molecular weight)/(UiO-66-AZODC mass fraction/UiO-66-AZODC molecular weight),

where the AZODC mass fraction = 12.5%, AZODC Mw = 270.24 g/mol, UiO-66-AZODC mass=100%, UiO-66-AZODC unit coordinated with one molecule of AZODC ($Zr_6C_{60}H_{38}O_{33}N_2$), Mw=1862.28 g/mol. Please note that this molecular formula is in an ideal condition, but in a real case, for MOFs with defects, the formula would be different.

The calculated molar ratio of AZODC is about 0.86. This means that one MOF unit shares ~0.86 AZODC molecule, which is close to the above suggested one-AZODC coordinated MOF molecular structure.

## 2. Supplementary Tables

Table S1. Examples of on-off ratio in AZO-based light-gated nanochannels or subnanochannels

| On-off ratio | Materials | Target compound(s) | Reference |
|---|---|---|---|
| 4.8 | Zeolite-AZO membrane | Gas | 1 |
| 1.3 | AZO-protein voltage-gated channel | $K^+$ ion | 2 |
| 2.1 | AZO modified protein channel | Ions | 3 |
| 5 | AZO-P6A host-guest nanochannel | $K^+$ ion | 4 |
| 3.3 | AZO-PDDA nanochannel | Ions | 5 |
| 1.3 | AZO-UiO-66 PIM-1 mixed-matrix membrane | Gas | 6 |
| 16.7 | AZO-dimeric complex membrane | $Cl^-$ ion | 7 |
| 17.8 | AZO-confined UiO-66 subnanochannel | $Li^+$ ion | 8 |
| 40.2 | UiO-66-AZODC subnanochannel | $Li^+$ ion | This work |

Table S2. EDX results of MOF crystals

(a) EDX results of UiO-66 crystals

| Element | Mass Norm. [%] | Atom [%] | Abs. error [%] (1 sigma) | Rel. error [%] (1 sigma) |
|---|---|---|---|---|
| Carbon | 43.13 | 71.47 | 0.93 | 12.58 |
| Oxygen | 13.89 | 17.28 | 0.35 | 14.73 |
| Zirconium | 41.43 | 9.04 | 0.29 | 4.10 |
| Nitrogen | 1.55 | 2.21 | 0.10 | 36.20 |

(b) EDX results of UiO-66-AZODC-2:1 crystals

| Element | Mass Norm. [%] | Atom [%] | Abs. error [%] (1 sigma) | Rel. error [%] (1 sigma) |
|---|---|---|---|---|
| Carbon | 33.37 | 61.95 | 0.66 | 13.82 |
| Oxygen | 15.22 | 21.22 | 0.34 | 15.45 |
| Zirconium | 48.25 | 11.80 | 0.28 | 4.12 |
| Nitrogen | 3.16 | 5.03 | 0.13 | 29.55 |

According to the N contents by EDX results, it can be concluded that the N content originated from AZODC is about **1.61%** (obtained by 3.16%-1.55%). Then, we calculated the N contents from the above hypothesized one AZODC coordinated with one cavity of UiO-66, using the following equation:

$$\text{N content} = \text{N mass}/\text{UiO-66-AZODC mass} \times 100\% =$$

$$(14.01\ \text{g/mol} \times \text{mole number})/(1862.28\ \text{g/mol} \times \text{mole number}) \times 100\%$$

The molar ratio between N and UiO-66-AZODC unit is 2:1, then the final N content in the UiO-66-AZODC unit is calculated to be 1.5%. This calculated result is very close to the EDX result of **1.61%,** indicating that the UiO-66-AZODC mostly consists of UiO-66 with one AZODC. Please note that EDX offers element content of a limited region of the sample instead of expressing the elementary compositions of the whole sample, this may be the reason that causes the differences.

References


1. K. Weh, M. Noack, K. Hoffmann, K. P. Schroder and J. Caro, *Microporous Mesoporous Mater.*, 2002, 54, 15-26.
2. A. Mourot, M. A. Kienzler, M. R. Banghart, T. Fehrentz, F. M. Huber, M. Stein, R. H. Kramer and D. Trauner, *ACS Chem. Neurosci.*, 2011, 2, 536-543.
3. A. Rullo, A. Reiner, A. Reiter, D. Trauner, E. Isacoff and G. Woolley, *Chem. Commun.*, 2014, 50, 14613-14615.
4. Y. Sun, J. Ma, F. Zhang, F. Zhu, Y. Mei, L. Liu, D. Tian and H. Li, *Nat. Commun.*, 2017, 8, 260.
5. K. Y. Chun, Y. J. Son, S. Jo and C. S. Han, *Small*, 2018, 14, 1703618.
6. N. Prasetya and B. P. Ladewig, *J. Mater. Chem. A*, 2019, 7, 15164-15172.
7. M. Ahmad, S. Metya, A. Das and P. Talukdar, *Chem. Eur. J.*, 2020, 26, 8703-8708.
8. T. Qian, H. Zhang, X. Li, J. Hou, C. Zhao, Q. Gu and H. Wang, *Angew. Chem. Int. Ed.*, 2020, 59, 13051-13056.